

REMARKS

Claims 1 and 4-30, as amended, remain in the present application for the Examiner's review and consideration. Claims 2, 3, 31 and 32 have been canceled from consideration with the present application without prejudice to pursue the subject matter of these claims in one or more continuation or divisional applications. Claim 1 has been amended to include the recitations of claims 2 and 3 as originally filed, and support for this amendment is found in claims 2 and 3. As this amendment does not introduce any new matter into the present application, its entry at this time is warranted. Claim 25 has been amended to correct a typographical error.

Examiner's courtesy extended to the Applicant and his representative during the Interview on 11 April 2006 is greatly appreciated.

Claims 1-15, 20, 21, 24, 26, 27, 31 and 32 were rejected under 35 U.S.C. § 102(b) as anticipated by or, in the alternative, under 35 U.S.C. § 103(a) as obvious over U.S. patent no. 5,624,729 to Cohen et al. ("Cohen") for the reasons given on pages 2-3 of the Office Action. It was asserted that Cohen discloses or renders obvious all of the limitations of these claims. Cohen was said to disclose a composite fabric comprising an elastic sheet and a fibrous pile inserted into the elastic sheet by stitch-bonding. The fibrous materials were said to be nonelastic fibers, and the elastic films were said to be stretchable in both dimensions. It was admitted that Cohen does not explicitly teach the limitations of elastic recovery of the composite, elastic modulus and shrinkage. These limitations were presumed to be inherent to the present invention or in the alternative to be obvious in view of Cohen. Applicant respectfully asserts that the claims as presently amended overcome this rejection.

Cohen is directed to a composite elastic material having *an increased pile density*. The composite elastic material is made by a method which includes the step of inserting substantially individualized fibrous materials into an *elongated* elastic sheet by stitch-bonding (col. 4, lines 60-63). Cohen discloses that the elastic sheet should be elongated at least about 15 percent, for example, from about 20 to about 400 percent and maintained in that elongated condition while the individualized fibrous materials, such as a carded batt of staple fibers, are attached to the elastic sheet (col. 5, lines 9-14). The elastic sheet may be an elastic film or an elastic nonwoven web of fibers (col. 5, lines 23-24).

The individualized fibrous materials may be nonelastic fibers or batts or nonelastic fiber bundles. It is worthwhile to note Cohen defines "non-elastic" to include materials that can stretch up to 125% of its unstretched length and can recover at least 40% of the elongation (col. 2, lines 25-42.)

If the fibrous materials are fiber bundles, they may be, for example, threads, yarns, or multifilament strands (col. 5, lines 48-49 and 54-56). Fiber bundles may be used with equipment such as, for example, tufting machines or stitch-bonding machines which individually insert the fiber bundles into the stretched elastic sheet by tufting processes or stitch-bonding processes (col. 9, lines 62-66).

By contrast as presently recited in claim 1, the present invention is directed to a stitch-bonded elastic composite containing a non-fibrous elastic sheet stitch-bonded in a substantially unstretched state with substantially inextensible yarns. Cohen is silent on stitching in an unstretched state, because doing so would not increase the “pile density”, which is at the center of the invention in the Cohen reference.

In addition, claim 1 recites that the stitch-bonded substantially inextensible yarns form a stitched yarn network that allows stretch beyond as-stitched dimensions of 10-100%, in at least one direction. In contrast, Cohen fails to teach or disclose that the stitched yarn network allows stretch beyond the as-stitched dimensions. Cohen mainly discusses inserting individual fibers into a stretched substrate by mechanical needling and allowing the substrate to relax to increase the pile density. Mechanical needling is a different process than stitch-bonding in that needling does not form a stitched yarn network. To the extent that specific combinations are presented, the examples illustrated in Tables 1 and 2 compare mechanical needling of an unstretched conventional non-woven substrate and of a stretched non-woven substrate, and not stitch-bonding as claimed. The portions of Cohen that discuss stitch-bonding are silent on stretching beyond the as-stitched dimensions, because such stretch is not desirable bearing in mind that Cohen’s purpose is to increase the pile density, not decreasing it by stretching beyond the as-stitched dimensions.

Regarding the suggestion that the present invention is inherent from the disclosure of Cohen, there is no disclosure directed to the inherent properties that would assist one of ordinary skill in the art to make composites having the properties of the present invention. Applicant respectfully submits that Cohen does not disclose stitch-bonding a substantially unstretched elastic film with substantially inelastic yarns to allow it to stretch beyond the as-stitched dimensions. The Cohen reference cares about increasing pile density, but the claimed invention does not. Cohen and the present invention are directed to different end products prepared by opposite processes, *i.e.*, Cohen’s stretching the substrate during stitching bonding to increase pile density when the tension on the substrate is released versus the present invention’s stitch bonding an unstretched elastic film with substantially inextensible yarns to allow stretch beyond the as-stitched dimensions.

“In relying upon the theory of inherency, the examiner must provide a basis in fact and/or technical reasoning to reasonably support the determination that the allegedly inherent characteristic necessarily flows from the teachings of the applied prior art.” *Ex parte Levy*, 17 USPQ2d 1461, 1464 (Bd. Pat. App. & Inter. 1990) (emphasis in original). As discussed above, there is no factual or technical reason that claim 1, as amended, would necessarily flow from the applied prior art.

Hence, amended claim 1 is believed to be novel and un-obvious over the Cohen reference. Claims 2-15, 20, 21, 24, 26 and 27 depend on claim 1 and are also presently patentable.

Claims 1-4, 10-16, 18, 20, 21, 27 and 29-32 were rejected under 35 U.S.C. § 102(b) as anticipated by or, in the alternative, under 35 U.S.C. § 103(a) as obvious over U.S. patent no. 5,826,905 to Tochacek et al. (“Tochacek”) for the reasons given on pages 4-5 of the Office Action. It was asserted that Tochacek discloses a stitch-bonded fabric having a thermoplastic base web and a stitching yarn knitted through the thermoplastic base (column 1, lines 52 - 60). The thermoplastic base layer can be an elastomeric film or a laminate of an elastomeric film and nonwoven layer (column 4, lines 10-15). The stitching yarn is made from polyamide or polyester yarns (column 2, lines 53 - 56). The stitch construction can be a chain stitch or tricot stitch pattern (column 3, lines 15 - 40). As shown in the figures the stitch pattern is an open pattern which would allow the backing to be seen through the yarn overlaps. The thermoplastic base layer can have a basis weight of 50 to 175 grams (column 4, lines 25 - 30). Further, the elastomeric material would have some stretch in both directions. Although Tochacek was said to not explicitly teach the limitations of the elastic recovery of the entire composite, elastic modulus, and shrinkage, these limitations were presumed inherent to the invention. Support for said presumption was said to be found in the use of similar materials (*i.e.*, elastomeric film base layers) and in the similar production steps (*i.e.* stitch-bonding the film layer with nonelastic yarns) used to produce the composite fabric.

As presently recited in amended claim 1, the present invention is directed to a stitch-bonded elastic composite that has an elastic modulus in the stretch direction of less than about 400 grams per centimeter width per 10% stretch and that can stretch beyond the as-stitched dimension, *inter alia*. The disclosure of Tochacek is directed to fabrics suitable for airbag applications (see Abstract) and to the properties that make these fabrics more desirable for such applications, *i.e.*, burst strength and permeability. There is no teaching of suggestion regarding the stretch of these fabrics beyond the as-stitched dimensions or of the elastic modulus *per se*.

Regarding the suggestion that the present invention is inherent from the disclosure of Tochacek, there is no specific indication as to how the disclosure of Tochacek would inherently lead to the composite of the present invention. In fact, the desired burst strength and permeability of the airbag materials in general are more likely to lead one of ordinary skill in the art away from the composites of the present invention. As illustrated in following graph from the paper "A Study on the Modeling Technique of Airbag Cushion Fabric", by Soongu Hong of Hyundai MOBIS (attached herewith), the force displacement curve for airbag materials is significantly different than that of the composite of the present invention.

It is instructive to compare the claimed elastic modulus of 400 grams per centimeter width per 10% stretch to Figure 2 of the Hong paper, which Applicant submits represents

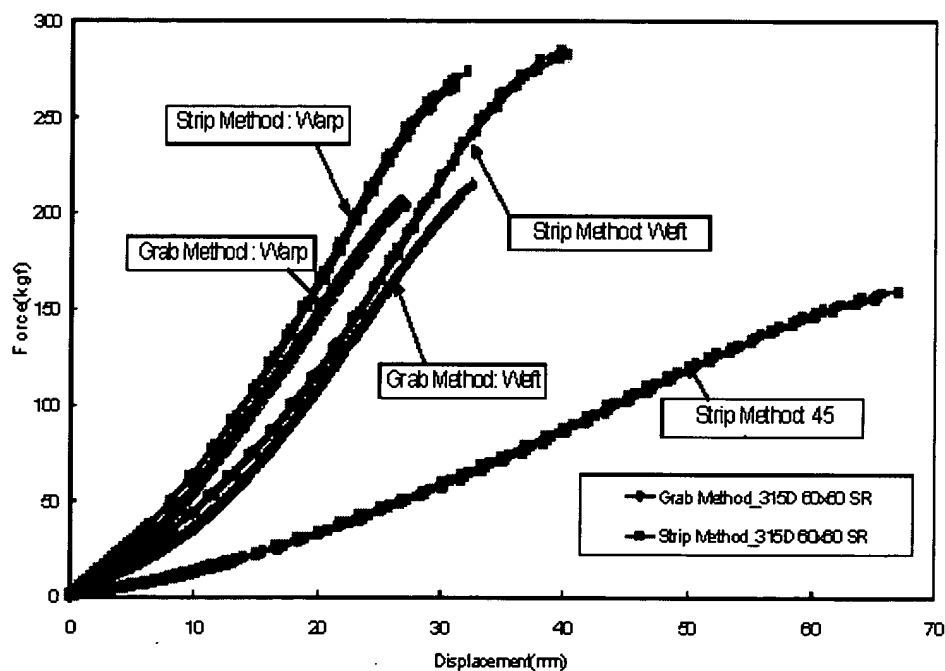


**Figure 2 Comparison graph between Grab and Cut Strip Method of 315 Denier 60x60 Silicon Coating**

objective evidence showing the elastic modulus of air bag materials. This Figure shows the force displacement curves for airbag fabrics measured with both a Grab test device on a specimen size of 76mm x 25.4mm, (or about 3" x 1"), and a Cut Strip test device on a specimen size of 76mm x 50mm (or about 3" x 2"). The Young's Modulus or elastic modulus is indicated by the slope of the force displacement curve.

The applied force reported by Hong for a 10% stretch (i.e., 7.6 mm stretch of a 76 mm sample) in a single direction, *i.e.*, warp or weft, by both test methods is about 25-50 kg (force). The lowest curve on this graph appears to be the diagonal stretch direction (45° to warp and weft) and shows a force of about 10-12 kg for 10% stretch. The width of the sample also does not appear to change the results significantly at lower loads, except for the diagonal direction. The force required to stretch airbag materials 10% (25-50 kgf or 10-12kgf) is significantly greater than the force required to stretch composites of the present invention (0.4 kg) by about one order of magnitude, and, hence, the stitch-bonded elastic composite of the present invention would not necessarily flow from the disclosure of Tochacek. Therefore, one of ordinary skill in the art given the disclosure of Tochacek would not recognize the composite of the present invention as necessarily present and would not anticipate success in making the composite of the present invention.

Hence, claim 1 is patentable over the Tochacek reference and claims 2-4, 10-16, 18, 20, 21, 27 and 29-30 depend on claim 1 and are also presently patentable.

Claims 5-9 were rejected under 35 U.S.C. §103(a) as being unpatentable over Tochacek in view of Cohen for the reasons given on page 5 of the Office Action. Claims 22 and 23 were rejected under 35 U.S.C. § 103(a) as being unpatentable over Cohen or Tochacek for the reasons given on pages 5-6 of the Office Action. Claim 16 was rejected under 35 U.S.C. § 103(a) as being unpatentable over Cohen in view of Tochacek for the reasons given on page 6 of the Office Action. Claim 17 was rejected under 35 U.S.C. § 103(a) as being unpatentable over Tochacek for the reasons given on pages 6-7 of the Office Action. Claim 19 was rejected under 35 U.S.C. § 103(a) as being unpatentable over Cohen for the reasons given on page 7 of the Office Action. Applicant notes that claims 5-9, 16, 17, 19, 22 and 23 depend either directly or indirectly from claim 1 and contain additional recitations that further define the present invention over Cohen and Tochacek either alone or in combination. Hence these claims are also currently patentable due to their dependency, and Applicant believes that it is unnecessary to address these specific grounds of rejection of the dependent claims at this time. However, Applicant reserves the right to address these rejections should that become necessary.

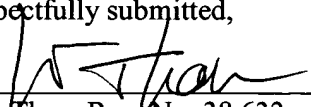
Claims 24 - 26 were rejected under 35 U.S.C. § 103(a) as being unpatentable over Tochacek in view of U.S. patent no. 5,376,430 to Swenson et al. ("Swenson") for the reasons given on page 8 of the Office Action. Claim 25 was rejected under 35 U.S.C. 103(a) as being unpatentable over Cohen in view of Swenson for the reasons given on pages 8-9 of the Office Action. The shortcomings of Tochacek and Cohen are not overcome by Swenson. Swenson

is directed to non-tacky, multi-layer elastomeric laminates comprising at least one elastomeric core layer and at least one relatively nonelastomeric skin layer. Claims 24-26 depend either directly or indirectly from claim 1, and as was discussed above, the current recitations of claim 1 are neither anticipated or rendered obvious as inherent in the disclosure of Tochacek and Cohen either alone or in combination.

Claim 28 was rejected under 35 U.S.C. § 103(a) as being unpatentable over Cohen in view of U.S. patent no. 1,253,050 to Kitsee for the reasons given on page 9 of the Office Action. It was asserted that Kitsee discloses that pile fabrics can be provided with a design by cutting or shearing the surface of the fabric, which would create an embossed design (page 1, lines 10-15) and that it would have been obvious to add a design as disclosed by Kitsee, to the pile fabric taught by Cohen et al. to make the fabric more visually appealing. As asserted by the Examiner, Kitsee does not remedy the deficiencies of Cohen vis-à-vis amended claim 1. Claims 28 depends directly from claim 1, and as was discussed above, the current recitations of claim 1 are neither anticipated or rendered obvious as inherent in the disclosure of Cohen. Therefore, claim 28 is not rendered obvious by reference to Cohen in view of Kitsee.

Applicant asserts that all claims are now in condition for allowance, early notice of which is respectfully requested. If the Examiner believes, for any reason, that personal communication will expedite prosecution of this application, the Examiner is invited to telephone the undersigned at the number provided.

A petition for one-month extension of time is attached herewith. No other fees are believed due in connection with the submission of this Amendment. If any fee is due, the Commissioner may charge appropriate fees to H.T. Than Law Group, Deposit Account No. 50-1980.

Respectfully submitted,  
  
\_\_\_\_\_  
H.T. Than, Reg. No. 38,632  
Attorney for Applicant

Date: 11 April 2006

The H.T. Than Law Group  
Waterfront Center  
1010 Wisconsin Avenue, N.W.  
Suite 560  
Washington, DC 20007  
Telephone: (202) 363-2620  
Facsimile: (202) 363-2620

# A Study on the Modeling Technique of Airbag Cushion Fabric

Soongu Hong

Applied Technology Research Dept., Hyundai MOBIS

## ABSTRACT

The decision of linear elastic Young's Modulus and other properties of airbag cushion fabric is difficult mainly due to the non-linearity of stress-strain curve of cushion fabric. Especially for the tensile test of cushion fabric, the different test methods add complexity in determining proper linear elastic modulus. Poisson's ratio has been generally assumed as a mean value of steel's one and rubber's one in the modeling of airbag cushion in previous researches.

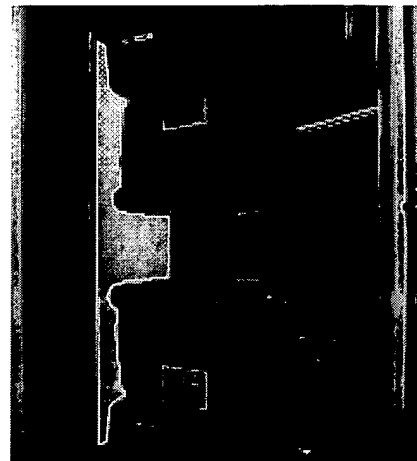
In this study, airbag droptower test and simulation were performed to find the proper material properties of airbag cushion fabric such as Young's Modulus, Poisson Ratio, Permeability and Shear Modulus. By modeling the textile cushion fabric material type as isotropic and orthotropic material with linear and nonlinear membrane element, the material properties of cushion fabric with which numerical analysis shows good agreements with droptower test were found. i-SIGHT optimization program has been applied in optimization phase. The DOE (Design Of Experiment) analysis results of cushion fabric material properties are presented.

## INTRODUCTION

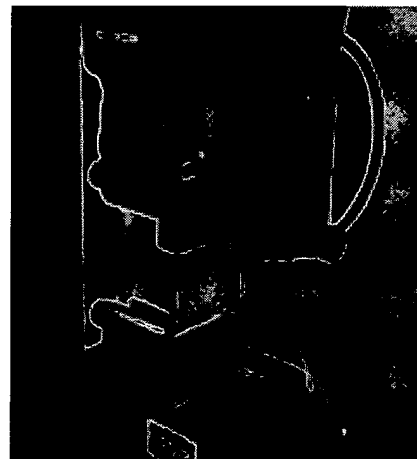
Mostly, MADYMO airbag model uses the linear or nonlinear membrane element that consists of 3-node triangular element at the airbag cushion fabric modeling. And assuming the cushion fabric material type as elastic material, the material properties such as isotropic linear, isotropic tension material, orthotropic linear material and orthotropic tension material was used at the airbag cushion fabric modeling<sup>(1,2)</sup>.

It is extremely difficult to evaluate exact properties of airbag cushion fabric such as Young's Modulus, Poisson's Ratio, Air Permeability Coefficient and Shear Modulus. J.J Nieboer et. al. used averaged value of warp, weft and 45 degree of weft cushion fabric's Young's Modulus as representative value. Poisson's Ratio of 0.4 which is mean value of steel's and rubber's has been adopted as a representative value<sup>(3)</sup>. One of the reasons why it is difficult to have consistent material properties of cushion fabric comes to the varieties of test methods. Young's modulus of cushion fabrics is being

measured by largely two methods, one is Cut strip Method and the other is Grab Method<sup>(4)</sup>.



(a) Grab Method



(b) Cut Strip Method

Figure 1 Cushion fabric tensile test set-up conditions of Grab and Cut Strip Method

## TEST METHODOLOGY

The structures of grip of two tensile test methods are shown in Figure 1. Figure 1 (a) shows Grab test device where the specimen size is 76 mm x 25.4mm. Figure 1 (b) shows Cut Strip test<sup>(5)</sup> device where the specimen size is 76 mm x 50mm. Figure 2 shows an example of Force- Displacement curves (FD curve) of cushion fabric which were measured with both test methods. The Young's Modulus, the slope of non-linear FD curve, can be quite arbitrary with regard to the point where slope is evaluated.

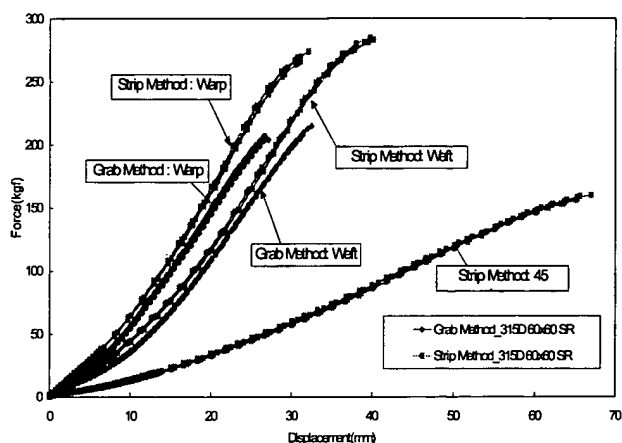


Figure 2 Comparison graph between Grab and Cut Strip Method of 315 Denier 60x60 Silicon Coating

Into the bargain, the way to measure the total section area of cushion fibers, which is indispensable for the evaluation of stress, has a choice between thickness measurement of airbag yarn and the microscopic analysis of warp and weft.

Tensile test of 4-type 420 denier cushion fabrics has been conducted with Grab method and Cut strip methods. Each test has been repeated 5 times for the stable acquisition of test data. Table 1 shows Young's Modulus of tested fabrics. Last column of Table 1 lists Young's Modulus which has been assessed with TNO Cut Strip Method, where warp, weft direction and 45 degree of warp direction Young's modulus are averaged.

As shown in Figure 2, the Cut Strip Method shows stiffer FD curve than Grab Method. This difference can be attributed to the wider width of Cut Strip Method specimen than that of Grab Method. The tensile test to warp direction of cushion fabric brought stiffer FD curve than the tensile test to weft direction, because of the difference of weaving pattern. Figure 2 also shows the non-linearity of FD curve, which adds difficulties in determining Young's Modulus of fabric. No specific relationship between Grab and Cut Strip method can be found either in Figure 2.<sup>(4)</sup>

A constant value of Poisson's Ratio can only be calculated with FD curve using linear elastic assumptions.

Table 1 Young's Modulus values regarding Grab and Cut Strip Method (Unit: N/m<sup>2</sup>)

	Grab Method	Cut Strip Method	Cut Strip (***)
49X49Uncoated	1.331E+9	7.234E+8	5.478E+8
49X49Si coated	9.756E+8	6.106E+8	4.592E+8
46X46Si coated	1.005E+9	7.731E+8	5.678E+8
57X52Uncoated	1.304E+9	6.792E+8	5.259E+8

(\*\*\*) This is TNO Cut Strip Method that averaged values in warp weft and 45 degree of warp direction are arranged.

The permeability of airbag cushion can be measured by test, however the accuracy and repeatability of the test are low. The permeability data can be incorporated into MADYMO model as the pressure-time curve or air permeability-pressure curve. The application of simpler type permeability, constant coefficient, needs trial and error method for the correlation of test data. As for the shear modulus, it is impossible to measure in cushion fabric.

In this paper, airbag droptower test and simulation were performed to find the proper material properties of airbag cushion fabric such as Young's Modulus, Poisson Ratio, Permeability and Shear Modulus. By modeling the textile cushion fabric material type as isotropic and orthotropic material with linear and nonlinear membrane element, the material properties of cushion fabric with which numerical analysis shows good agreements with droptower test were found. i-SIGHT optimization program has been applied in optimization phase. The DOE (Design Of Experiment) analysis results of cushion fabric material properties are presented.

## MODEL AND TEST

To obtain the proper material properties of airbag fabric such as Young's Modulus, Poisson's Ratio, Permeability, Shear Modulus, etc, and relationship among the variables, the droptower test of driver airbag was conducted and the MADYMO model was constructed. Before the droptower simulation, the deflection simulation of cantilever beam was conducted to find out the suitable optimization methodology for non-linear problem. Consequently, the optimization of material properties was conducted to minimize the difference between test and simulation results, resulting in the proper material properties that can be applied in numerical analysis. The relationship of the various variables of cushion fabric and test results has been studied too.

## DROPTOWER TEST METHODOLOGY

After the driver airbag module was fastened to steering wheel, steering wheel is fixed to droptower base plate



(mass: 34.75kg). The droptower height and airbag firing time had been set so as the droptower surface may coincide with the fully deployed airbag surface in free fall state. The driver airbag without cover and platen cushion (non-folding) has been tested. The front panel of airbag cushion was coated and the rear panel was uncoated. The detailed airbag specification is shown in Table 2. The deceleration, force, displacement of droptower and airbag firing time were measured. The droptower test set-up and its results were shown in Figure 3.

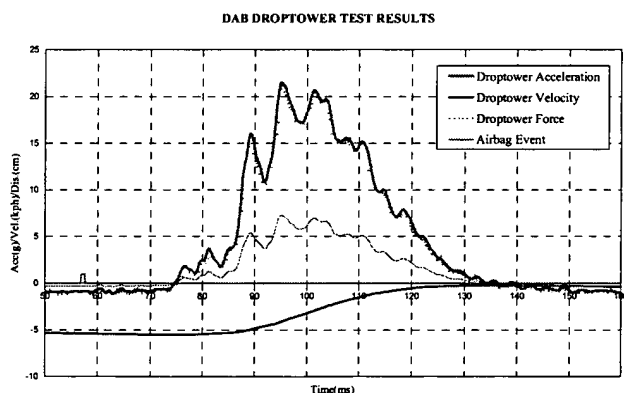
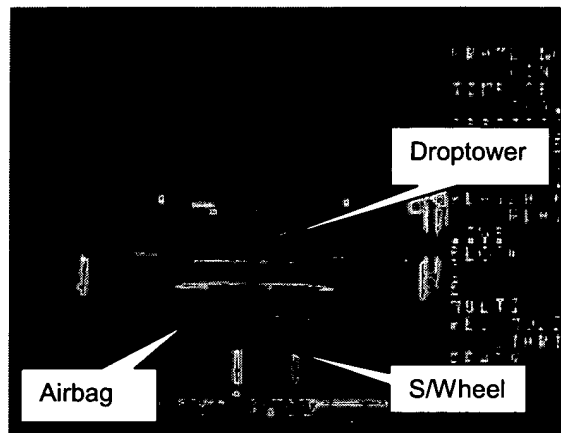


Figure 3 Droptower test set-up and test results

## MADYMO MODELING OF DROPTOWER

The droptower model consists of bracket joint, translational joint, one ellipsoid, four cylinders, twelve planes. Steering wheel system consists of four translational joints, four revolute joints and 35 ellipsoids. Airbag model FE data has been constructed with BAGGEN. The droptower MADYMO model and simulation result are shown in Figure 4.

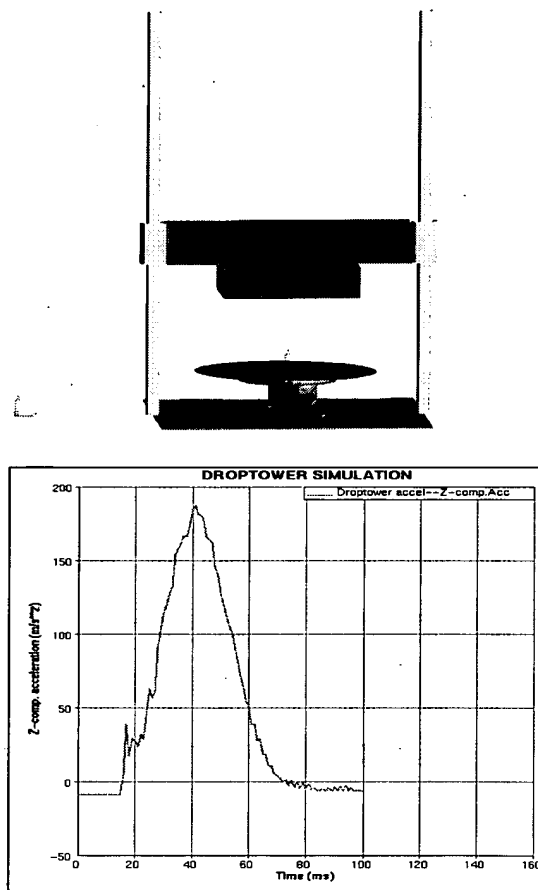


Figure 4 Droptower model and simulation result

Table 2 Driver airbag specifications for droptower test

Material	Parameter	Variable	Unit	Value
Airbag Cushion Front (Si coated 420D 49x49)	Thickness	T	Mm	0.0279
	Density	P	Kg/m3	761
Airbag Cushion Rear (Uncoated 420D 57x52)	Thickness	T	mm	0.0302
	Density	P	Kg/m3	660
Strap (Si coated 420D 46x46)	Width		mm	20mm
	Thickness		mm	0.0279
Tether	Number	n	-	4
Tether Length	Initial Length	L0	mm	296

## DROPTOWER OPTIMIZATION PROCESS

### Pre-optimization results of cantilever beam example

For the application of most appropriate optimization technique among various internal i-SIGHT<sup>(6)</sup> optimization techniques, a pre-optimization for the deflection simulation of cantilever beam was conducted. These optimization results are shown in Table 3.

The Latin Hypercube was applied in prior to each five optimization technique. Table 3 shows that the Hooke–Jeeves Pattern Search method gives the best correlation between test and simulation in non-linear cantilever beam problem. As a result, Hooke–Jeeves Pattern Search method has been selected for the optimization of droptower airbag simulation.

### Optimization process of droptower :

The optimization process consists of parameter parsing, MADYMO run, output parsing and data analysis phase. At first, the input parameters such as Young's Modulus, Poisson's Ratio, Permeability, Shear Modulus and strap stiffness of airbag front panel and rear panel were read at input parsing phase. (Figure 5) Also the separated window was opened to compare the graph between test and simulation pulse.

The optimization ranges of each airbag parameter are shown in Table 4.

Table 4 The Range of variables to run Latin Hyper Cube and optimization

Airbag Cushion Variable	Range
Permeability Rear Panel	0~1
Poisson's Ratio of Front and Rear Panel	0.0~0.5
Young's Modulus of Front and Rear Panel	2.0E+8~3.0E+9
Tether Stiffness	3700~56600

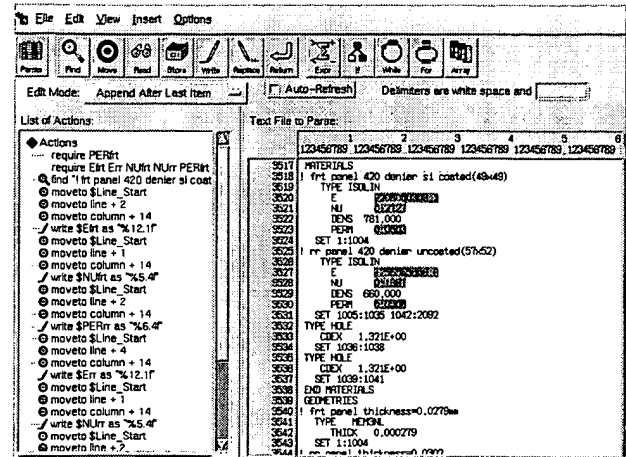


Figure 5 i-SIGHT parameter input parsing process of MADYMO input data

After a set of MADYMO run is completed, the droptower Z-acceleration results were read at the output parsing phase for the comparison of the test and simulation. Last is data analysis phase, the optimization was conducted by minimizing the object function given in equation (1)

$$OBJ = \sum_{i=1}^n (|Rti - Rsi|) \quad (1)$$

Where, Rti : Test acceleration, Rsi : Simulation acceleration.

### Optimization result of droptower

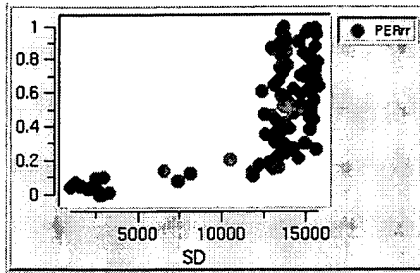
In the Table 4, after Latin Hypercube was run twice to minimize the range of parameter, Hooke–Jeeves Pattern Search method for optimization has applied at droptower simulation. The detailed results and DOE results were attached at Appendix. Only permeability of these results were shown in Figure 6~Figure 12.

Table 3 Correlation results of deflection for cantilever beam

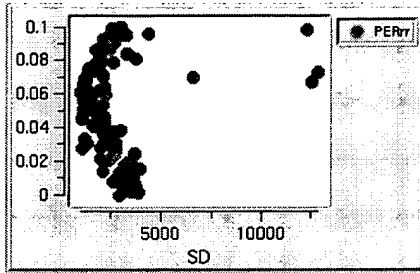
	Initial Value	Solution	SLP*	EP*	NLPQL*	SA*	HJ*
Gradient Step			0.01	0.01	0.01	0.01	0.01
Step Size Reduction Factor							0.5
Termination Step Size							1.0E-3
Object (Sum of Deviation)			<b>31.433</b>	<b>12.385</b>	<b>11.009</b>	<b>18.642</b>	<b>1.434</b>
Design Variable	TLF1**	5.0	2.0	2.0120	2.099	2.052	1.990
	TLF2**	4.0	4.0	3.369	4.820	4.807	3.523
	DAS1**	1.0	6.0	5.6910	5.958	5.972	5.799
	DAS2**	3.0	3.0	2.784	2.197	1.269	2.183
	ME**	5.1E+10	7.1E+10	7.5E+10	6.7E+10	6.9E+10	7.3E+10

\*SLP : Sequential linear programming, EP : Exterior Penalty, NLPQL : Sequential Quadratic Programming, SA : Simulated Annealing, HJ : Hook-Jeeves Pattern Search

\*\* TLF1 : Tabled Force 1, TLF2 : Tabled Force 2, DAS1 : Data Scaling1, DAS2 : Data Scaling2

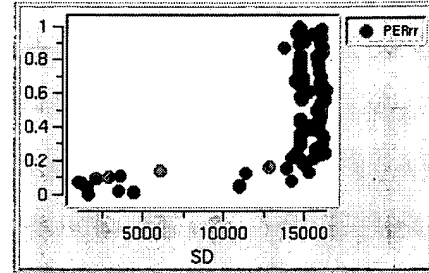


a) Permeability (0~1)

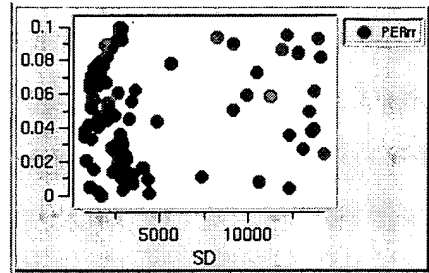


b) Permeability (0~0.1)

Figure 6 Results of Latin Hyper Cube-Isotropic linear material (200 run)



a) Permeability (0~1)



b) Permeability (0~0.1)

Figure 8 Results of Latin Hyper Cube-Isotropic tension material (200 run)

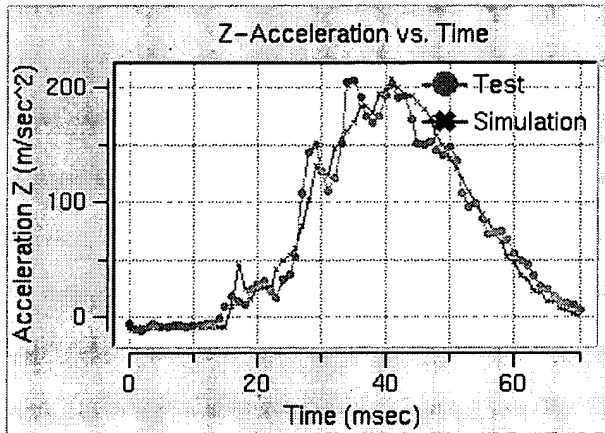


Figure 7 Optimization result of droptower test correlation (Isotropic linear material)

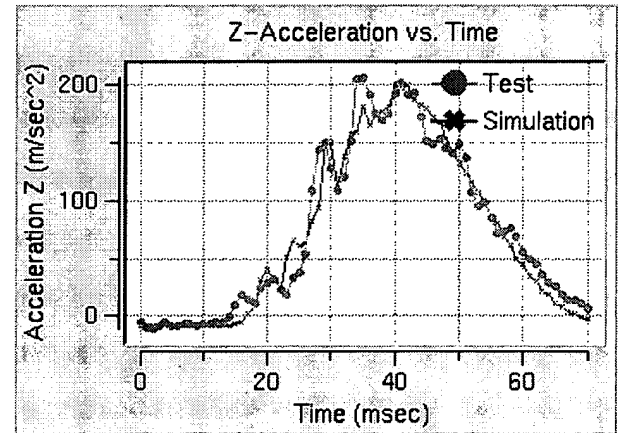


Figure 9 Optimization result of droptower test correlation (Isotropic tension material)

Table 5 Optimization results of airbag cushion material properties (Isotropic linear material)

Run	PERrr	Efrt	Err	Nufrt	NUrr	STIFF	SD	Type
132	0.0503	2.28E+9	2.566E+8	0.2386	0.165	56600	778.9	MEM3
143	0.0503	2.21E+9	2.566E+8	0.441	0.16667	56600	725	MEM3NL

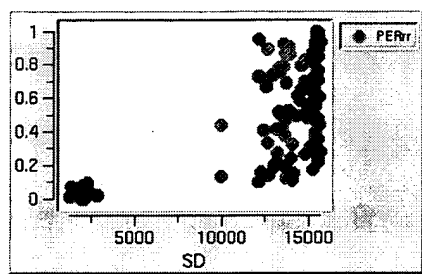
Table 6 Optimization results of airbag cushion material properties (Isotropic tension material)

Run	PERrr*	Efrt*	Err*	Nufrt*	Nurr*	STIFF*	SD*	Type
240	0.034343	2.406E+9	1.16E+9	0.895	0.075	27783	786.4	MEM3
286	0.0322	3.0E+9	1.447E+9	0.0444	0.076	27783	930	MEM3NL

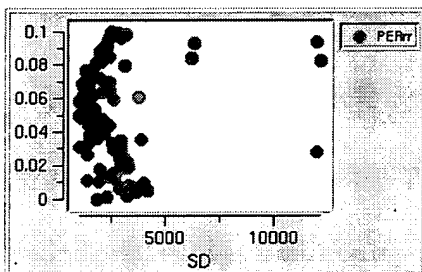
\* PERrr : Permeability of cushion rear panel, Efrt, Err : Young's Modulus of front and rear panel, Nufrr, Nurr : Poisson's Ratio of cushion front and rear panel, STIFF : Stiffness of tether, SD : Sum of deviation between test and simulation, MEM3, MEM3NL : Membrane 3 node element of linear and nonlinear

Table 7 Range of variables to run Latin Hyper Cube and optimization of orthotropic linear material

Airbag Cushion Variable	Range
Permeability Rear Panel	0~1
Poisson's Ratio of Front and Rear Panel	0.0~0.5
Young's Modulus of Front and Rear Panel	2.0E+8~3.0E+9
Shear Modulus of 1-2 Direction of Cushion	6.667E+8~1.5e+9
Tether Stiffness	3700~56600



a) Permeability (0~1)



b) Permeability (0~0.1)

Figure 10 Results of Latin Hyper Cube-Orthotropic linear material (200 run)

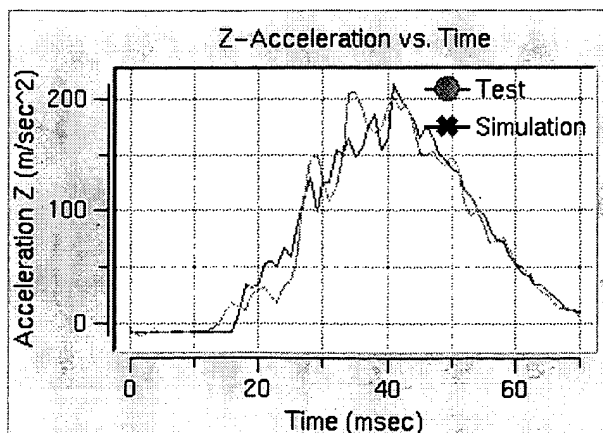
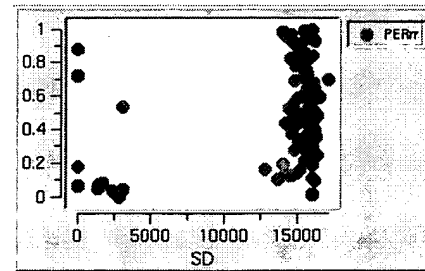
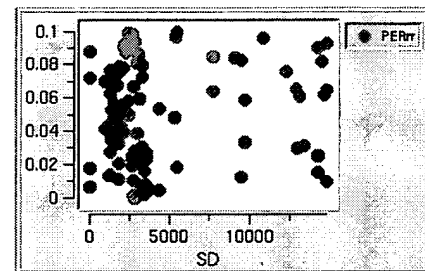


Figure 11 Optimization result of droptower test correlation (orthotropic linear material)



a) Permeability (0~1)



b) Permeability (0~0.1)

Figure 12 Results of Latin Hyper Cube-orthotropic tension material

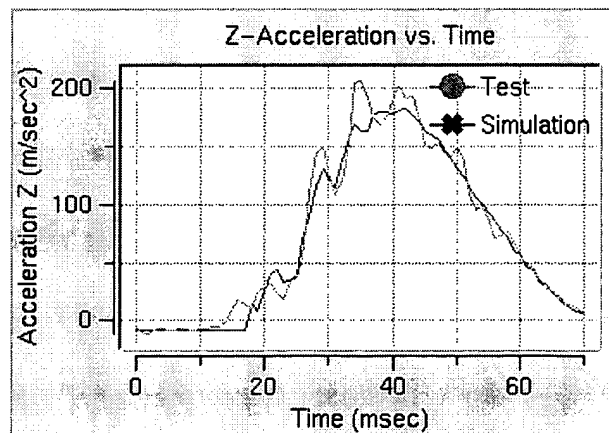


Figure 13 Optimization result of droptower test correlation (orthotropic tension material)

## DISCUSSION AND RESULTS

As shown in Table.5, 6, 8, 9, the case of membrane 3 node element and orthotropic tension material model shows lowest object function value, which means best correlation between test and simulation. However, the

application of membrane 3 node element and orthotropic tension material model needs more assumption in airbag modeling than simpler isotropic tension material model.

Therefore, It's recommended that the membrane 3 element and isotropic tension material model should be applied in airbag modeling.

Table 8 Optimization results of airbag cushion material properties (orthotropic linear material)

Run	E11ft	E22ft	NU12ft	G12ft	E11rr	E22rr
401	1.558E+9	1.727E+9	0.11616	1.39E+8	2.236E+8	2.321E+9
	Nu12rr	G12rr	PERrr	STFF	SD	Type
	0.2323	1.196E+9	0.0313	9640	820.4	MEM3
Run	E11ft	E22ft	NU12ft	G12ft	E11rr	E22rr
419	1.558E+9	1.727E+9	0.11616	1.043E+8	2.236E+8	2.321E+9
	Nu12rr	G12rr	PERrr	STFF	SD	Type
	0.465	1.196E+9	0.0313	9640	823.4	MEM3NL

Table 9 Optimization results of airbag cushion material properties (orthotropic tension material)

Run	E11ft*	E22ft*	NU12ft*	G12ft*	E11rr*	E22rr*
456	3.0E+9	6.31E+8	0.05808	1.39E+8	2.24E+9	2.32E+9
	Nu12rr*	G12rr*	PERrr*	STFF*	SD*	Type
	0.0	1.2E+9	0.0313	9640	608	MEM3*
Run	E11ft	E22ft	NU12ft	G12ft	E11rr	E22rr
499	1.56E+9	1.73E+9	0.137	1.39E+8	2.787E+9	2.32E+9
	Nu12rr	G12rr	PERrr	STFF	SD	Type
	0.465	1.196E+9	0.0355	9640	877.4	MEM3NL*

\* PERrr : Permeability of cushion rear panel, E11ft, E22ft : Young's Modulus of 1 and 2 direction of front cushion panel, E11rr, E22rr : Young's Modulus of 1 and 2 direction of rear cushion panel NU12ft, NU12rr : Poisson's Ratio of 1, 2 direction of front and rear cushion panel, G12ft, G12rr : Shear Modulus of 1, 2 direction of front and rear cushion panel, STIFF : Stiffness of tether, SD : Sum of deviation between test and simulation, MEM3, MEM3NL : Membrane 3 node element of linear and nonlinear

Linear membrane 3 node element type gave better correlation results than Non-linear membrane 3 node element type except the case where isotropic linear material model was applied. It was found that the optimized Young's Modulus value is above 1.0E+9. With regard to the material properties applied in airbag analysis, the Grab Method can be said to give more proper Young's modulus than the Cut Strip Method.

Latin Hyper Cube simulation shows that no airbag cushion parameter but airbag permeability has relationship with test results. DOE analysis also shows that the effect of permeability was largest through Latin Hyper Cube simulation as shown in Table 10, Appendix. The permeability effect of orthotropic material model was lower than that of isotropic material model.

## CONCLUSION

Optimization process has been applied to simulation data correlation process. Consequently, following conclusions have been found.

From a Latin Hyper Cube simulation, no airbag cushion parameter but airbag permeability has been found to has relationship with test results.

It's recommended that the membrane 3 node element, isotropic tension material type should be applied in airbag

cushion fabric modeling. The isotropic tension material can be used with a little assumption than orthotropic tension material.

## ACKNOWLEDGMENTS

The authors greatly appreciate a support of W.J. Park, Engineous Korea to develop the optimization program and analysis.

## REFERENCE

1. MADYMO USER'S MANUAL 3D Version5.4.1, p101~123.
2. MADYMO THEORY MANUAL Version5.4, p108~112.
3. J.J. Nieboer, J.Wismans, and P.J.A de Co, "Airbag Modeling Techniques", SAE902322, TNO Road-Vehicles Research Institute, Delft, Netherlands 1990
4. Standard Test Method for Breaking Strength and Elongation of Textile Fabrics (Grab Test), ASTM D 5034-95, KS K 0520
5. Standard Test Method for Breaking Force and Elongation of Textile Fabrics (Strip Method), ASTM D 5035-95, KS K 0521
6. i-SIGHT MANUAL
7. Horst Vogt, "Dynamic Air Permeability Testing-An Important New Tool"

## CONTACT

[sghong1@mobis.co.kr](mailto:sghong1@mobis.co.kr), [soonguhong@yahoo.co.kr](mailto:soonguhong@yahoo.co.kr)

Senior Research Engineer

Applied Technology Dept. Hyundai MOBIS Korea

## APPENDIX

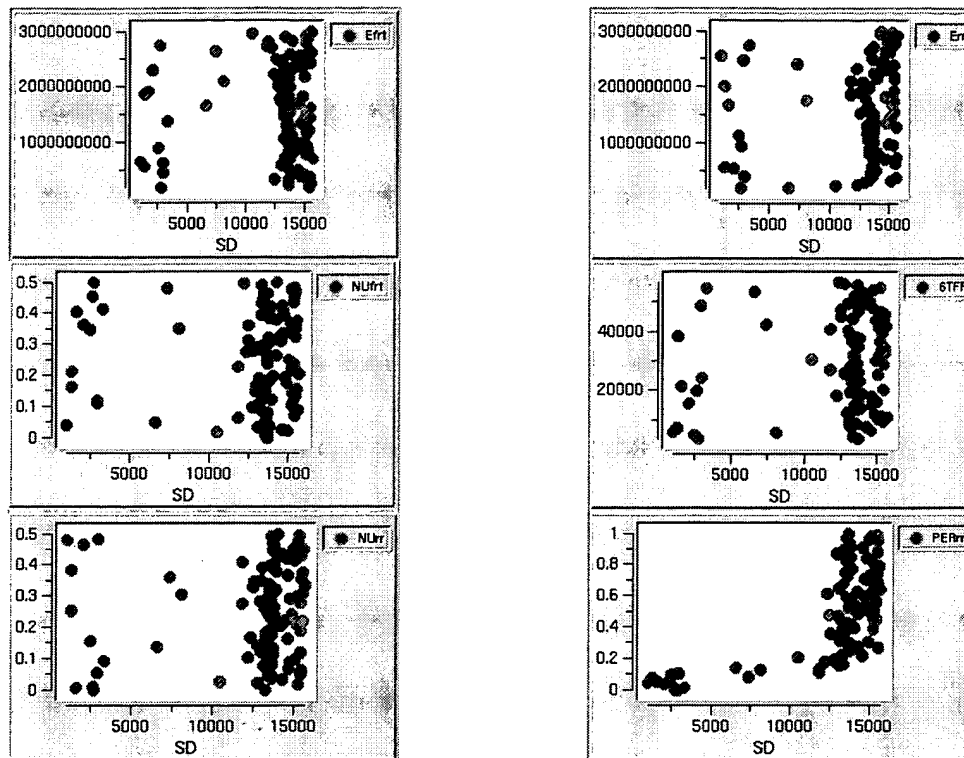


Figure 14 Results of Latin Hyper Cube (100 run)-Permeability (0.0~1)

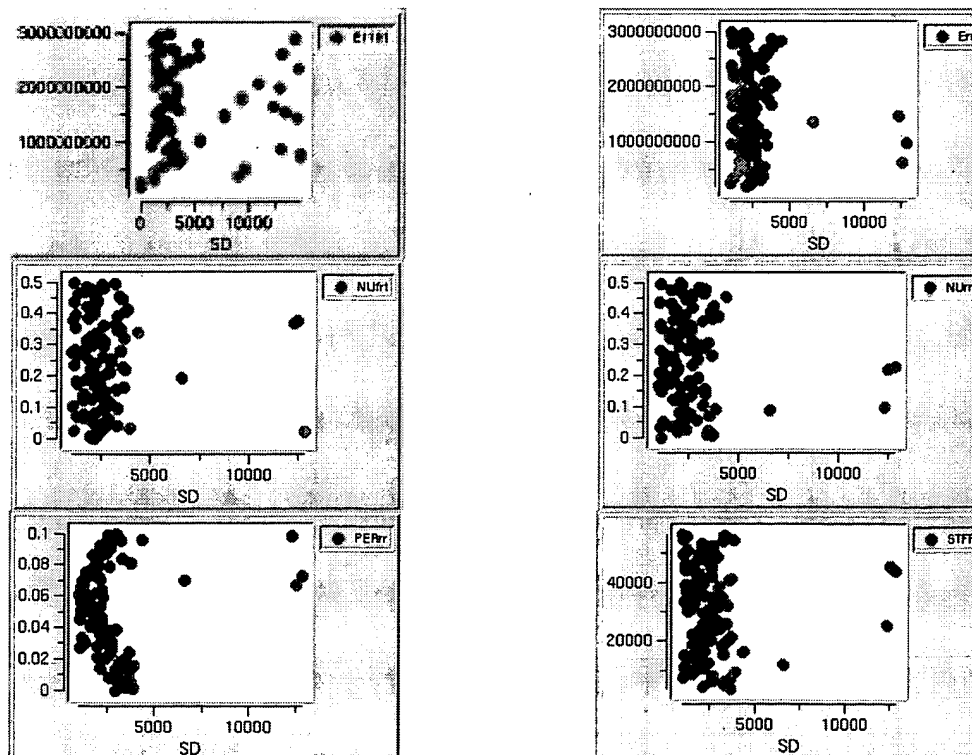


Figure 15 Results of Latin Hyper Cube (100 run)-Permeability (0~0.2)

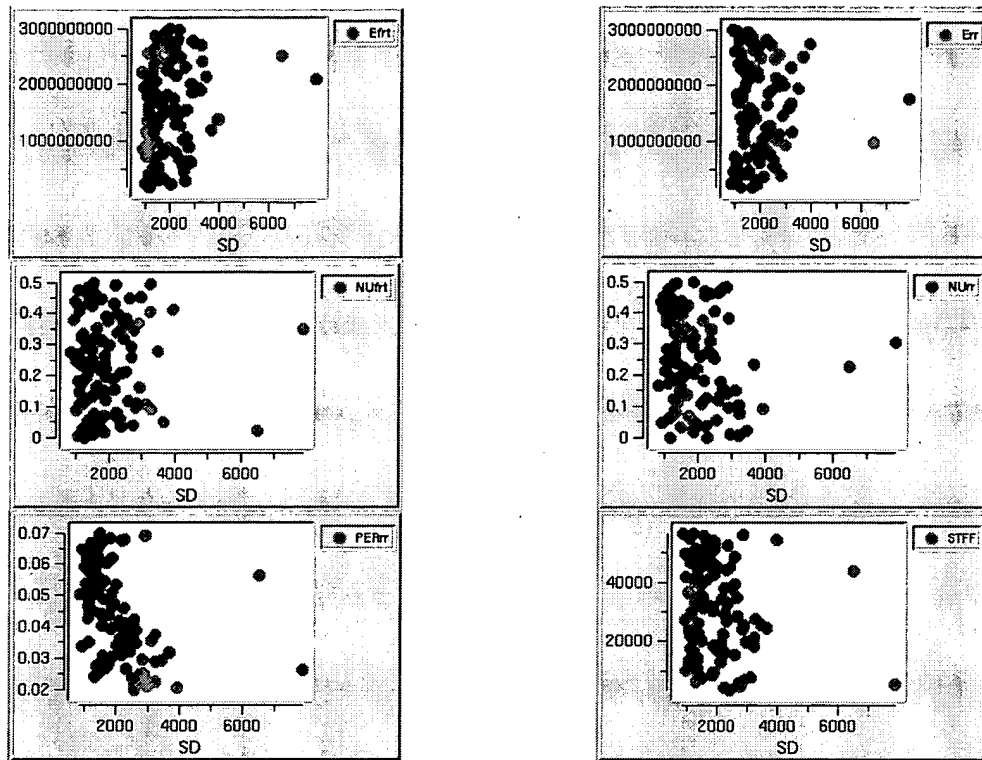


Figure 16 Results of Latin Hyper Cube (100 run)-Permeability (0.02~0.07)

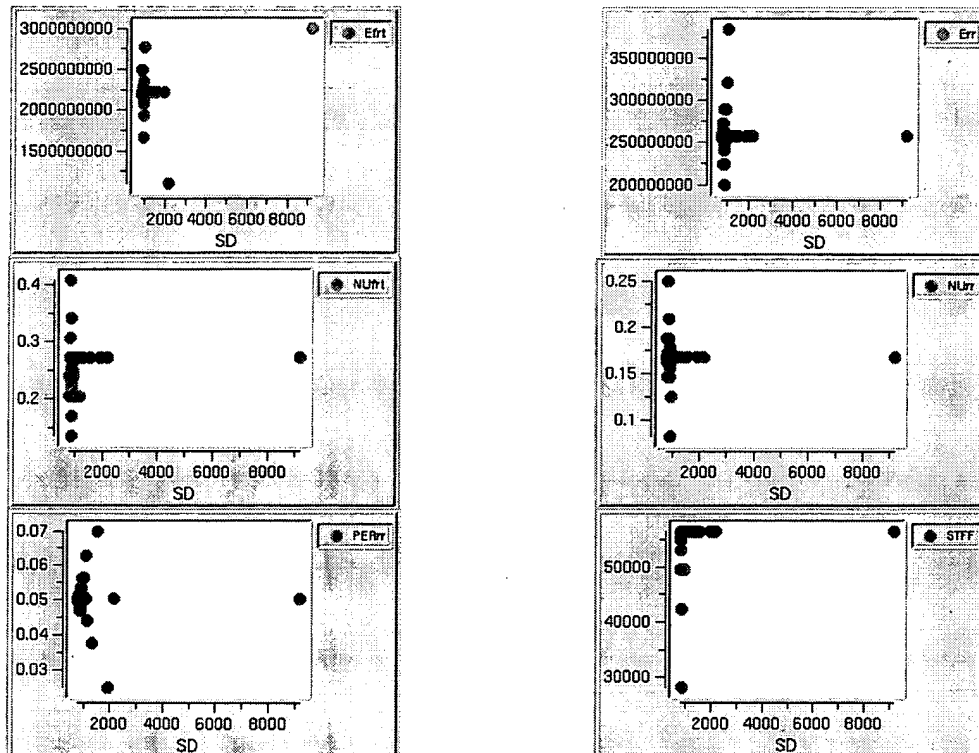
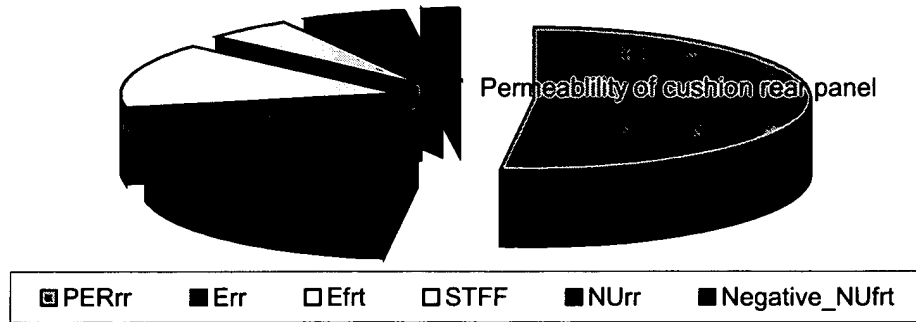
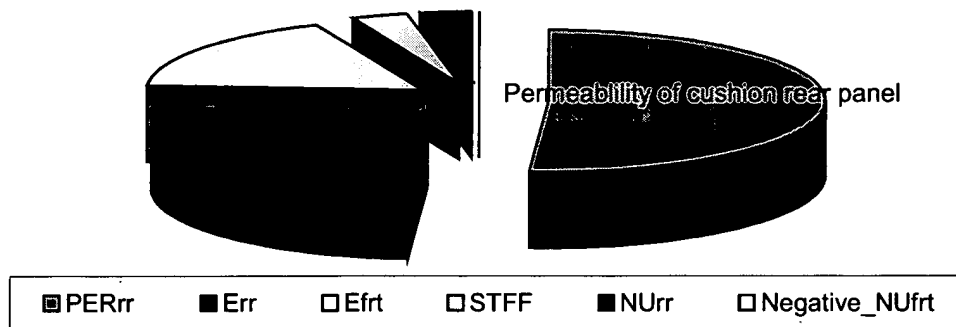


Figure 17 Result of Hook and Jeeves Pattern search (141 run)-Permeability (0.02~0.07)

Main effect of each variables (MEM3, isotropic linear material)



Main effect of each variables (MEM3, isotropic tension material)





Main effect of each variables (MEM3, orthotropic linear material)

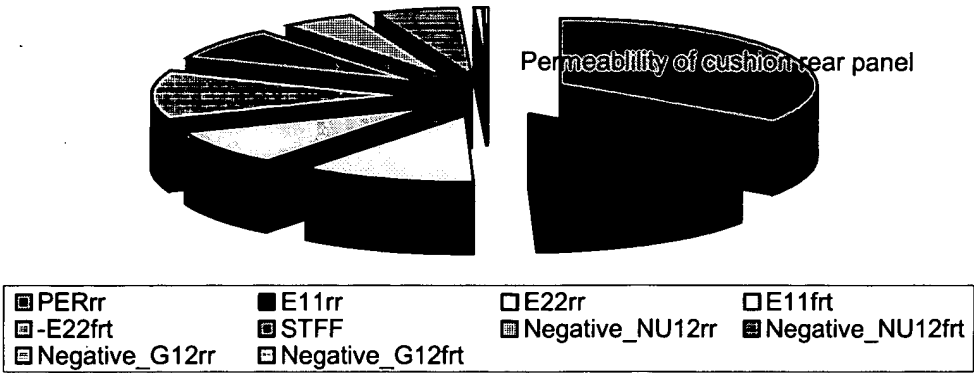


Table 10 Main effect analysis results of Latin Hyper Cube simulation

**This Page is Inserted by IFW Indexing and Scanning  
Operations and is not part of the Official Record**

**BEST AVAILABLE IMAGES**

Defective images within this document are accurate representations of the original documents submitted by the applicant.

Defects in the images include but are not limited to the items checked:

- ☐ **BLACK BORDERS**
- ☐ **IMAGE CUT OFF AT TOP, BOTTOM OR SIDES**
- ☐ **FADED TEXT OR DRAWING**
- ☐ **BLURRED OR ILLEGIBLE TEXT OR DRAWING**
- ☐ **SKEWED/SLANTED IMAGES**
- ☐ **COLOR OR BLACK AND WHITE PHOTOGRAPHS**
- ☐ **GRAY SCALE DOCUMENTS**
- ☐ **LINES OR MARKS ON ORIGINAL DOCUMENT**
- ☐ **REFERENCE(S) OR EXHIBIT(S) SUBMITTED ARE POOR QUALITY**
- ☐ **OTHER:** \_\_\_\_\_

**IMAGES ARE BEST AVAILABLE COPY.**

**As rescanning these documents will not correct the image problems checked, please do not report these problems to the IFW Image Problem Mailbox.**